

Fracture Mechanics Investigation of 18 Ni Maraging Steel Weldments

J. G. Blauel und H. Smith
Institut für Festkörpermechanik, Freiburg

G. Schulze
Schweißtechnische Lehr- und Versuchsanstalt, Berlin

This program, sponsored by the AIF/DVS, was conducted in response to the continued interest in what happens to the strength and toughness of high strength steels subjected to welding.

Materials Apparatus and Procedure

For our study 10 mm thick plates of maraging steel, X2 Ni Co Mo 18 9 5 (corresponding to the American steel 18 Ni grade 300 maraging) were selected. This material develops a strength of about 210 Kp/mm^2 and a plane strain fracture toughness of about $250 \text{ Kp/mm}^{3/2}$ when aged at 480°C for 3 to 8 hours.

Welding was performed by the TIG process using rods of composition similar to that of the base material (fig.1). When working with extreme cleanliness and applying the parameters of fig.1, a good joint was obtained as judged by radiographic inspection.

During welding, time-temperature cycles for heating and cooling were measured at various points in the HAZ. Subsequently, these were reproduced by a SMIT-weld simulator in specimens 10 x 10 mm in cross section. From the rather large number of time-temperature cycles actually "seen" by the HAZ of a multilayered weldment, we selected five with peak temperatures of 650, 700, 750, 800 and 1350°C because of their critical influence on

on grain size and formation of retained austenite. For strength and toughness testing of the joint as well as the uniform microstructures, round bar tensile ($\phi = 4$ mm) and three point bend specimens (10x10x55 mm) were used. For this, special fixtures and a clip gauge were developed and installed in a MTS machine. Fatigue precracks were carefully located in metallographic zones of interest made visible by polishing and etching the side surface of the specimen containing the weld. Fracture toughness testing was then conducted in accordance with ASTM recommendations.

For fracture mechanics testing, the effect of nonuniformity of the mechanical properties throughout the weld has to be taken into account. The results of a linear elastic stress analysis by RATWANI (fig.2) show that for typical values of the elastic moduli of the HAZ and the melted zone, and for a small value $h/a = 0.5$, the deviation from the stress intensity factor of the homogeneous material is negligibly small.

The size of the plastic zone was estimated according to IRWIN's model to be proportional to the factor $(K_I / \sigma_{o,2})^2$. Representative average values of the yield stress $\sigma_{o,2}$ taken from tensile experiments were used to check the validity of our K_{IC} results.

Residual stress influences were not observed in this program, probably due to the combination of small specimen size, crack orientation and postweld aging.

Extensive metallography by light microscope was performed and scanning electronmicroscope fractographs were taken as required. Stable austenite was determined by x-ray diffraction with prior austenite grain size being determined by the intercept method.

Results

To obtain a uniform grain size distribution of the base material a simple re-solution annealing investigation was performed at different temperatures. The microstructures and the mechanical properties are shown in fig. 3. The 845°C treatment appears to embrittle the material, while at 900°C the toughness is restored.

The weld joint was analysed in terms of three areas of interest:

- (a) the fusion zone
- (b) the transformed zone
- (c) the dark band zone

The microstructures and the measured properties are shown in fig. 4.

The dark band zone consists of transformed martensite with large amounts of stable austenite formed along discrete planes in the grains. The strength values decrease while the fracture toughness increases. All critical dimensions were valid except for crack lengths which were only slightly too short. The transformed zone shows the expected austenite grain size. Only a small reduction of K_{IC} compared with the base material values is noted. The melted zone was very brittle in spite of the pools of stable austenite seen here. This particular morphology together with the high titanium content probably accounts for the low toughness.

The effect of simulated weld cycles on the re-solution annealed base material is shown in fig.5. The 650 and 700°C treatments resulted in fairly high stable austenite contents with the microstructure being similar to that observed in the dark band zone of the weldment. The fracture toughness is correspondingly high (Again here the crack lengths were a little too short).

The 750 and 800°C treatments stabilized very little austenite, but resulted in decreased toughness in a manner similar to the 845°C solution annealing treatment previously described. This slight embrittling effect was not found in the transformed zone of the weldment although the microstructures appear to be the same as observed here. The 1350°C treatment developed very large prior austenitic grains although the fracture toughness was not greatly different than that of the parent material.

Zusammensetzung des Versuchswerkstoffs (W) und der Schweißstäbe (St)

	C	Si	Mn	P	S	Al	Co	Mo	Ni	Ti
W	0,004	0,02	0,02	0,005	0,004	0,085	9,05	4,94	17,8	0,79
St	0,004	0,02	0,02	0,006	0,006	0,120	8,80	4,80	18,2	0,98

fig.1:

Einstellwerte beim WIG-Schweißen (6 Lagen)

Strom I = 195-210 Amp.
 Spannung U = 13-15 Volt
 Vorschubgeschwindigkeit v = 0,13-0,18 cm/sec (letzte Lage: 0,09 cm/sec)
 Energiezufuhr Q = 14,1-24,2 KJ/cm (letzte Lage: 35 KJ/cm)

Chemical composition of material (W) and weldrods (St)
 Welding parameters

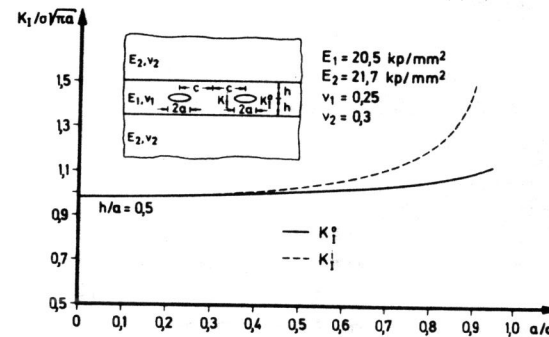


fig.2:

Stress intensity factor at the inner (K_I^i) and the outer crack tip (K_I^o) as a function of the reciprocal crack distance a/c in a three layered medium

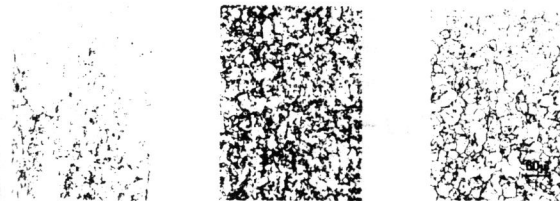
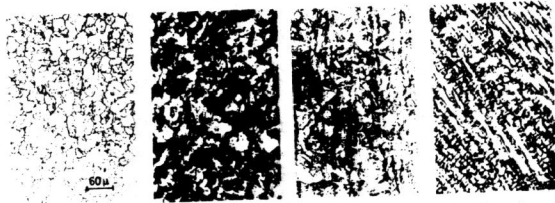


fig.3:

Microstructure, average grain size, and fracture toughness of the base material after different solution annealing treatments.

Wärmebehandlung:	(820°C/30'/Luft)	(820°C/30'/Luft) (845°C/30'/Luft) (480°C/4h/Luft)	(820°C/30'/Luft) (900°C/30'/Luft) (480°C/4h/Luft)
mittl. Korndurchmesser:	10-105 μ	10 μ	22 μ
Rißzähigkeit (TS-Proben):	$K_{Ic} = 255 \text{ kp/mm}^{3/2}$	$K_{Ic} = 183 \text{ kp/mm}^{3/2}$	$K_{Ic} = 245 \text{ kp/mm}^{3/2}$



Grundmaterial
 $Y_s < 1\%$
 $\phi = 22 \mu$
 $\sigma_{0.2} = 210 \text{ kp/mm}^2$
 $\sigma_B = 216 \text{ kp/mm}^2$
 $K_{Ic} = 246 \text{ kp/mm}^{3/2}$
 (TS-Proben)

Dunkelzone
 $Y_s = 3-50\%$
 $\phi = 22-27 \mu$
 $\sigma_{0.2} = 189 \text{ kp/mm}^2$
 $\sigma_B = 196 \text{ kp/mm}^2$
 $K_{Ic} = 287 \text{ kp/mm}^{3/2}$

Umwandlungszone
 $Y_s = 5-9\%$
 $\phi = 27-60 \mu$
 $\sigma_{0.2} = 209 \text{ kp/mm}^2$
 $\sigma_B = 214 \text{ kp/mm}^2$
 $K_{Ic} = 226 \text{ kp/mm}^{3/2}$

Schmelzzone
 $Y_s = 8-12\%$
 $\phi = 60-110 \mu$
 $\sigma_{0.2} = (181) \text{ kp/mm}^2$
 $\sigma_B = (182) \text{ kp/mm}^2$
 $K_{Ic} = 143-190 \text{ kp/mm}^{3/2}$

fig.4:
Microstructures and properties of different zones in a TIG weld joint



fig.5:
Simulated weld microstructures and their properties in HFX 760 after aging

σ_s [°C]	650	700	750	800	1350
Y_s [%]	12	21	8	5	2
ϕ [μ]	18	20	24	26	56
$\sigma_{0.2}$ [kp/mm ²]	186	182	209	216	202
σ_B [kp/mm ²]	191	188	215	223	206
K_{Ic} [kp/mm ^{3/2}]	300	323	182	211	221

VIII-431